Clinical Translation of a ^{68}Ga-Labeled Integrin $\alpha_v\beta_6$–Targeting Cyclic Radiotracer for PET Imaging of Pancreatic Cancer

Xun Feng[1], Yanpu Wang[1], Dehua Lu[1], Xiaoxia Xu[2], Xin Zhou[2], Huiyuan Zhang[2], Ting Zhang[1], Hua Zhu[2], Zhi Yang[2], Fan Wang[1], Nan Li[2], and Zhaofei Liu[1]

[1]Medical Isotopes Research Center and Department of Radiation Medicine, School of Basic Medical Sciences, Peking University Health Science Center, Beijing, China; and [2]Key Laboratory of Carcinogenesis and Translational Research (Ministry of Education/Beijing), Department of Nuclear Medicine, Peking University Cancer Hospital and Institute, Beijing, China

The overexpression of integrin $\alpha_v\beta_6$ in pancreatic cancer makes it a promising target for noninvasive PET imaging. However, currently, most integrin $\alpha_v\beta_6$–targeting radiotracers are based on linear peptides, which are quickly degraded in the serum by proteinases. Herein, we aimed to develop and assess a ^{68}Ga-labeled integrin $\alpha_v\beta_6$–targeting cyclic peptide (^{68}Ga-cycratide) for PET imaging of pancreatic cancer. **Methods:** ^{68}Ga-cycratide was prepared, and its PET imaging profile was compared with that of the linear peptide (^{68}Ga-linear-pep) in an integrin $\alpha_v\beta_6$–positive BxPC-3 human pancreatic cancer mouse model. Five healthy volunteers (2 women and 3 men) underwent whole-body PET/CT imaging after injection of ^{68}Ga-cycratide, and biodistribution and dosimetry were calculated. PET/CT imaging of 2 patients was performed to investigate the potential role of ^{68}Ga-cycratide in pancreatic cancer diagnosis and treatment monitoring. **Results:** ^{68}Ga-cycratide exhibited significantly higher tumor uptake than did ^{68}Ga-linear-pep in BxPC-3 tumor–bearing mice, owing—at least in part—to markedly improved in vivo stability. ^{68}Ga-cycratide could sensitively detect the pancreatic cancer lesions in an orthotopic mouse model and was well tolerated in all healthy volunteers. Preliminary PET/CT imaging in patients with pancreatic cancer demonstrated that ^{68}Ga-cycratide was comparable to ^{18}F-FDG for diagnostic imaging and postsurgery tumor relapse monitoring. **Conclusion:** ^{68}Ga-cycratide is an integrin $\alpha_v\beta_6$–specific PET radiotracer with favorable pharmacokinetics and a favorable dosimetry profile. ^{68}Ga-cycratide is expected to provide an effective noninvasive PET strategy for pancreatic cancer lesion detection and therapy response monitoring.

Key Words: pancreatic cancer; integrin $\alpha_v\beta_6$; ^{68}Ga radiotracer; PET/CT; cycratide

J Nucl Med 2020; 61:1461–1467
DOI: 10.2967/jnumed.119.237347

Pancreatic cancer is a highly deadly malignancy, characterized by strong invasion and high resistance to treatment (*1*). Most patients are diagnosed at the late stages of this disease, resulting in a 5-y survival rate of only 4%–8% (*2*). The current anatomic imaging modalities for pancreatic cancer care rely mainly on CT, MRI, and endoscopic ultrasound. Endoscopic ultrasound combined with fine-needle aspiration has a diagnostic sensitivity that ranges between 80% and 95% (*3*). However, this approach is relatively invasive and is dependent on experienced operators. Abdominal CT is most widely used to detect suspected pancreatic cancer, but it has limited sensitivity in the detection of tumors smaller than 2 cm (*4*). MRI has sensitivities and specificities in detecting and staging pancreatic cancers that are comparable to CT but may be more accurate in characterizing small subcentimeter lesions and metastases (*5*).

Compared with anatomic imaging modalities, molecular imaging techniques such as PET have advantages in providing functional and molecular information, which allows for early decision making in patients with pancreatic cancer (*4,6*). Currently, ^{18}F-FDG PET is the most commonly used technique in the clinic for initial assessment of disease progression and monitoring of treatment response. However, the use of ^{18}F-FDG has limitations, such as a lack of target-related specificity (*7,8*) and a broad differential diagnosis that includes conditions such as inflammation (*9*). Therefore, there remains a need to develop new PET radiotracers with high specificity for targeting malignant lesions and for differentiating malignant lesions from nonmalignant cysts.

Integrin $\alpha_v\beta_6$, a member of the integrin family, is closely related to the malignant behavior of a variety of tumors. In pancreatic cancer, the positive expression ratio of integrin $\alpha_v\beta_6$ is typically higher than 95% (*10,11*), making it a potential target for theranostics of pancreatic cancer. In the past several years, many peptide-based radiotracers have been developed for noninvasive PET (*12–17*) or SPECT (*18–20*) imaging of integrin $\alpha_v\beta_6$ in vivo. Most of the currently investigated integrin $\alpha_v\beta_6$–targeting peptides contain the RGDLXXL or DLXXL sequence (wherein X represents any undetermined amino acids), the major binding motif for integrin $\alpha_v\beta_6$ (*21*). Compared with antibodies, peptides possess advantages such as low cost, easy synthesis, and low immunologic reaction, which offer great potential for clinical use in nuclear medicine imaging. Recently, the ^{18}F-labeled A20FMDV2 peptide containing the RGDLQVL sequence was tested on human subjects. The safety, biodistribution, and radiation dosimetry of the

Received Sep. 25, 2019; revision accepted Feb. 10, 2020.
For correspondence contact either of the following: Zhaofei Liu, Medical Isotopes Research Center, Peking University, 38 Xueyuan Rd., Haidian District, Beijing 100191, China.
E-mail: liuzf@bjmu.edu.cn
Nan Li, Department of Nuclear Medicine, Peking University Cancer Hospital & Institute, Beijing 100142, China.
E-mail: rainbow6283@sina.com
Published online Feb. 21, 2020.

radiotracer (*17*), as well as its use in preliminary PET imaging in patients with malignant tumors (*13*), were assessed.

The preparation procedures for ^{18}F-labeled peptides are typically time-consuming and tedious, and equipment such as an on-site cyclotron is needed. By contrast, ^{68}Ga-labeled peptides can be prepared by kit formulation for rapid preparation of radiotracers for clinical use. Recently, integrin $\alpha_v\beta_6$–targeting peptides were radiolabeled with ^{68}Ga; the resulting radiotracers were tested on preclinical mouse models (*16*) and in clinical studies on PET imaging of non–small cell lung cancer (*22–24*). These pioneering studies demonstrated the potential of ^{68}Ga-labeled peptides targeting integrin $\alpha_v\beta_6$ for potential clinical use in cancer detection and treatment monitoring.

Our group previously developed a ^{99m}Tc-labeled linear peptide containing the RGDLATL sequence for integrin $\alpha_v\beta_6$–targeted SPECT imaging of pancreatic cancer and corresponding metastasis to the liver in mouse models (*20*). This integrin $\alpha_v\beta_6$–targeting peptide can also be modified for effective tumor-specific delivery of nanostructures and therapeutic agents (*11,25,26*). However, the linear peptide can be quickly metabolized in vivo after injection (*20*), limiting its further clinical translation. Cyclization has been proposed as a powerful strategy to improve the in vivo stability of peptides (*27,28*). As RGDLATL is the key sequence for integrin $\alpha_v\beta_6$ binding, we recently synthesized an RGDLATL-containing cyclic peptide by adding 2 cysteine residues at the N- and C-terminals to form a disulfide bridge. However, its integrin $\alpha_v\beta_6$–binding affinity was markedly reduced compared with the linear peptide (*29*). Therefore, in this study, we aimed to develop a new ^{68}Ga-labeled cyclic peptide based on the integrin $\alpha_v\beta_6$–targeting RGDLATL sequence. We evaluated the resulting radiotracer for its integrin $\alpha_v\beta_6$–specific tumor detection ability in animal models, assessed its biodistribution and dosimetry in healthy volunteers, and conducted clinical translational PET imaging in patients with pancreatic cancer.

MATERIALS AND METHODS

Synthesis of DOTA-Conjugated Peptides and ^{68}Ga Radiolabeling

The integrin $\alpha_v\beta_6$–targeting linear peptide RGDLATLKC (denoted as linear-pep) and the cyclic peptide cyclo[-RGDLATLK-] (denoted as cycratide) were custom-made by ChinaPeptides. Five micromoles of cycratide or linear-pep were mixed with 15 μmol of DOTA-*N*-hydroxysuccinimide-ester (Macrocyclics) in 300 μL of *N,N*-dimethylformamide. *N,N*-diisopropylethylamine was then added to the mixture so as to adjust the pH to 8.0–9.0. After 6 h of stirring at room temperature, the DOTA-conjugated peptides were isolated by high-performance liquid chromatography (HPLC). DOTA-cycratide was obtained in 60% yield, and its purity was determined by HPLC to be more than 95%. Matrix-assisted laser desorption/ionization time-of-light analysis revealed an m/z of 1,241.8 for $[MH]^+$ ($C_{53}H_{92}N_{16}O_{18}$; calculated molecular weight, 1,240.68). DOTA-linear-pep was obtained in 50% yield, the purity of which was determined by HPLC to be more than 95%. Matrix-assisted laser desorption/ionization time-of-light analysis revealed an m/z of 1,361.58 for $[MH]^+$ ($C_{56}H_{100}N_{18}O_{19}S$; calculated molecular weight, 1,360.71).

For ^{68}Ga radiolabeling, 10 nmol of DOTA-cycratide or DOTA-linear-pep were dissolved in 300 μL of NaOAc buffer and then reacted with 370–555 MBq of $^{68}GaCl_3$ for 10 min at 99°C. The reaction mixtures were then purified with Sep-Pak C18 cartridges (Waters) and passed through 0.22-μm Millipore filters into sterile multidose vials for further use. The radiochemical purity of the final products, ^{68}Ga-cycratide and ^{68}Ga-linear-pep, was determined by analytic HPLC.

Cell Culture and Animal Models

Integrin $\alpha_v\beta_6$–positive (*20*) BxPC-3 human pancreatic cancer cells were purchased from American Type Culture Collection. Cells were grown in RPMI-1640 medium (Invitrogen) supplemented with 10% fetal bovine serum at 37°C in a humidified atmosphere containing 5% CO_2.

All animal experiments were performed in accordance with the Guidelines of the Peking University Animal Care and Use Committee. Female BALB/c nude mice (5 wk old) were obtained from the Department of Laboratory Animal Science of Peking University. For the subcutaneous tumor model, 1×10^7 BxPC-3 cells were inoculated subcutaneously into the right flank of BALB/c nude mice. Tumor growth was measured with a caliper, and tumor volume was calculated using the following formula: volume = (length × width^2)/2. For the orthotopic tumor model, BALB/c nude mice were anesthetized, and small incisions were made in the abdomen of each mouse to expose the spleen. Next, 1×10^7 BxPC-3 cells in 50 μL of phosphate-buffered saline mixed with Matrigel (BD Biosciences) at a 1:1 ratio were injected into the pancreas, after which the incision was closed using sutures.

Cell-Binding Studies

In vitro integrin $\alpha_v\beta_6$–binding affinities of cycratide, DOTA-cycratide, and linear-pep were determined on BxPC-3 cells by a cell-binding assay. Because of the short half-life of ^{68}Ga, we used ^{64}Cu-labeled DOTA-cycratide (^{64}Cu-cycratide) as an alternative radioligand for ^{68}Ga-cycratide in the in vitro cell-binding assay. ^{64}Cu-cycratide was prepared using the same protocol as for ^{68}Ga-cycratide. The best-fit 50% inhibitory concentrations were calculated by fitting the data with nonlinear regression using Prism software (version 6.0; GraphPad Software).

The binding specificity of ^{68}Ga-cycratide to integrin $\alpha_v\beta_6$–positive BxPC-3 cells was also determined. Briefly, ^{68}Ga-cycratide (74 kBq) was added to cells cultured in 12-well plates with or without an excess (5 nmol) of cold cycratide and linear-pep peptides. After incubation at 4°C for 2 h, the cells were washed and collected. Cell-associated radioactivity was measured using a γ-counter (Packard). The result was expressed as the percentage of the total added dose per million cells.

Small-Animal PET Imaging

Each subcutaneous BxPC-3 tumor–bearing nude mouse was injected with 5.55 MBq (~0.19 μg) of ^{68}Ga-cycratide or ^{68}Ga-linear-pep with or without blocking doses of cold peptides via the tail vein ($n = 4$ mice per group). At 0.5, 1, and 2 h after injection, 10-min static PET scanning was performed using a small-animal PET/CT scanner (Mediso). For the blocking study, BxPC-3 tumor–bearing nude mice were coinjected with 50 mg of excess cycratide per kilogram of mouse body weight and 5.55 MBq of ^{68}Ga-cycratide, or a 50 mg/kg dose of linear-pep and 5.55 MBq of ^{68}Ga-linear-pep. Ten-minute static PET scans were then acquired at 0.5 h after injection (4 mice per group). PET images were analyzed, and the region-of-interest–derived percentage injected dose per gram of tissue (%ID/g) was calculated.

For PET imaging experiments with the orthotopic BxPC-3 tumor model, mice were injected with 5.55 MBq of ^{68}Ga-cycratide. At 0.5 h after injection, 10-min static PET scans were acquired. One day later, the same mice were coinjected with an excess dose of cold cycratide (50 mg/kg) and 5.55 MBq of ^{68}Ga-cycratide, and then PET imaging was performed at 0.5 h after injection. After PET scanning, the mice were euthanized, and the orthotopic tumor lesions were surgically excised. Half of each tumor was embedded in paraffin and then stained

with hematoxylin and eosin. The remaining half was frozen in optimal-cutting-temperature medium and cut into 5-μm-thick slices for immunofluorescence staining of integrin $\alpha_v\beta_6$.

Biodistribution Studies

Female BALB/c nude mice bearing subcutaneous BxPC-3 tumors were injected with 3.7 MBq of ^{68}Ga-cycratide or ^{68}Ga-linear-pep to evaluate the distribution of the radiotracer in the main organs (4 mice per group). The mice were euthanized at 0.5, 1, and 2 h after injection, and blood, tumor, main organs, and tissues were harvested, weighed, and measured using a γ-counter. For the blocking experiment, 4 tumor-bearing nude mice were administered 3.7 MBq of ^{68}Ga-cycratide along with an excess dose of cold cycratide (50 mg/kg). At 0.5 h after injection, all 4 mice were euthanized to determine organ biodistribution as described above.

In Vivo Metabolic Stability

Female BALB/c normal mice (3 mice per group) were injected with 37 MBq of ^{68}Ga-cycratide or ^{68}Ga-linear-pep via the tail vein. At 0.5 h after injection, mouse serum and urine samples were collected. After centrifugation, the supernatant was diluted with an aqueous solution of 50% acetonitrile, passed through a 0.22-μm Millipore filter, and analyzed by radio-HPLC.

Human Subjects

The Institutional Review Board of Peking University Cancer Hospital and Institute approved this study (approval 2018KT54), and all subjects gave written informed consent. Five healthy volunteers (2 women and 3 men; age range, 28–67 y; mean age ± SD, 46.2 ± 15.2 y) and 2 patients with suspected pancreatic cancer (1 woman and 1 man) were enrolled in this study.

PET/CT Procedures and Dosimetry in Healthy Volunteers

The 5 volunteers were deemed healthy on the basis of history, physical examination, electrocardiogram, urinalysis, and routine blood testing. No fasting or other special preparations were requested on the day of ^{68}Ga-cycratide PET/CT imaging. Any unusual or adverse clinical symptoms were recorded on the day of PET imaging and during the 2-wk follow-up period. All 5 volunteers underwent a low-dose CT scan (120 kV, 35 mA, slice thickness of 0.6 mm, pitch of 0.8, and matrix of 512 × 512) and then dynamic PET acquisitions using a Siemens Biograph mCT Flow 64 scanner at multiple time points from 0 min to 1 h after ^{68}Ga-cycratide injection (3.7 MBq/~0.12 μg/kg of body weight). The whole body of each subject (from the top of the skull to the middle of the femur) was covered by 6 bed positions, and the acquisition time was 40 s/bed position for the 5- and 15-min time points and 90 s/bed position for the 25-, 35-, 45-, and 60-min time points. One additional 10-min static PET image was also acquired at 2 h after injection.

A Siemens workstation (MultiModality Workplace) was used for data processing, and the PET images were reconstructed using ordered-subsets expectation maximization. Regions of interest for each normal organ were drawn manually by 2 experienced nuclear medicine physicians using 3-dimensional ellipsoid isocontours on each image with the correction of the corresponding CT images. The radioactivity concentrations (Bq/mL) of each organ and the single-voxel SUV in the volumes of interest were obtained through the Siemens workstation software.

The dosimetry calculation was performed using OLINDA/EXM 2.0 software (version 2.0; Hermes Medical Solutions AB). Briefly, the non–decay-corrected time–activity curve was generated according to the radioactivity concentrations (Bq/mL) of each organ. The time-integrated activity coefficient of each organ was determined by fitting the data using a biphase exponential model. The void time of the bladder was set as 60 min, and the absorbed doses were calculated by entering the time-integrated activity coefficient for all source organs into the software using the standard adult male (73.7 kg of body weight) and female (56.9 kg of body weight) phantoms.

PET/CT Imaging of Patients

Two patients underwent ^{68}Ga-cycratide PET/CT in a Siemens Biograph mCT Flow 64 scanner and ^{18}F-FDG PET/CT for comparison within 1 wk. A low-dose CT scan was used with the same parameters as described above. For ^{18}F-FDG PET/CT, the patients fasted for at least 6 h before intravenous injection of ^{18}F-FDG at a dose of 5.55 MBq/kg of body weight. ^{18}F-FDG/CT PET scans were performed 1 h after injection.

One patient (a 55-y-old woman) with suspected pancreatic cancer underwent whole-body PET/CT acquisitions at 1 h after ^{68}Ga-cycratide injection (3.7 MBq/~0.12 μg/kg), and the patient underwent surgical resection within 11 d after PET/CT imaging. Another patient (a 54-y-old man) with confirmed pancreatic cancer underwent PET/CT scanning 7 mo after surgery at 1 h after ^{68}Ga-cycratide injection (3.7 MBq/~0.12 μg/kg). Abdomen contrast-enhanced CT of this patient was performed within 2 wk of ^{68}Ga-cycratide scanning and was repeated for follow-up 3 mo later. The patient fasted for at least 6 h, and dual-phase contrast-enhanced CT scans (120 kV, 300 mA, tube rotation time of 1 s, 0.625-mm thickness with 0.625-mm gap, 36-cm field of view) were performed in a GE Lightspeed VCT (GE Healthcare) after intravenous administration of 100 mL of iohexol (300 mg I/mL) at a rate of 2.5–3.5 mL/s. The protocol during the acquisition period was at 30 s after iohexol administration for the arterial phase and 90 s for the portal venous phase.

Immunofluorescence Staining and Immunohistochemistry

The expression of integrin $\alpha_v\beta_6$ in tumor tissue was analyzed by immunofluorescence staining. Briefly, frozen tumor sections were fixed with ice-cold acetone for 10 min and then blocked with 1% bovine serum albumin (in phosphate-buffered saline) for 1 h. Then, tissues were incubated with mouse antihuman integrin $\alpha_v\beta_6$ antibody (clone E7P6; Chemicon/Millipore) for 1 h at room temperature and then visualized with fluorescent dye–conjugated secondary antibodies using a Leica TCS-NT confocal microscope.

For immunohistochemistry, paraffin-embedded tumor tissues from patients were deparaffinized. After endogenous peroxidase activity had been abolished using 0.3% hydrogen peroxide and antigen had been retrieved by microwave, tumor tissues were incubated with rabbit antihuman integrin $\alpha_v\beta_6$ antibody (bs-5791r; Bioss) overnight at 4°C. Afterward, tumor sections were incubated with a horseradish peroxidase–conjugated secondary antibody for 2 h and then were visualized by incubation with the diaminobenzidine substrate.

Statistical Analysis

The data were analyzed by GraphPad Prism software, version 6.0. One-way ANOVA and the unpaired Student *t* test were used for statistical analysis. *P* values of less than 0.05 were considered statistically significant.

RESULTS

Chemistry and Radiochemistry

The identity of DOTA-cycratide (Fig. 1A) and DOTA-linear-pep (Supplemental Fig. 1A; supplemental materials are available at http://jnm.snmjournals.org) were confirmed by mass spectroscopy. The decay-corrected labeling yield for ^{68}Ga-cycratide and ^{68}Ga-linear-pep ranged from 95% to 98%. After purification, the radiochemical purity of both radiotracers was more than 99%, with a specific activity of 37–55.5 MBq/nmol. Both ^{68}Ga-cycratide and ^{68}Ga-linear-pep showed favorable in vitro stability, with a

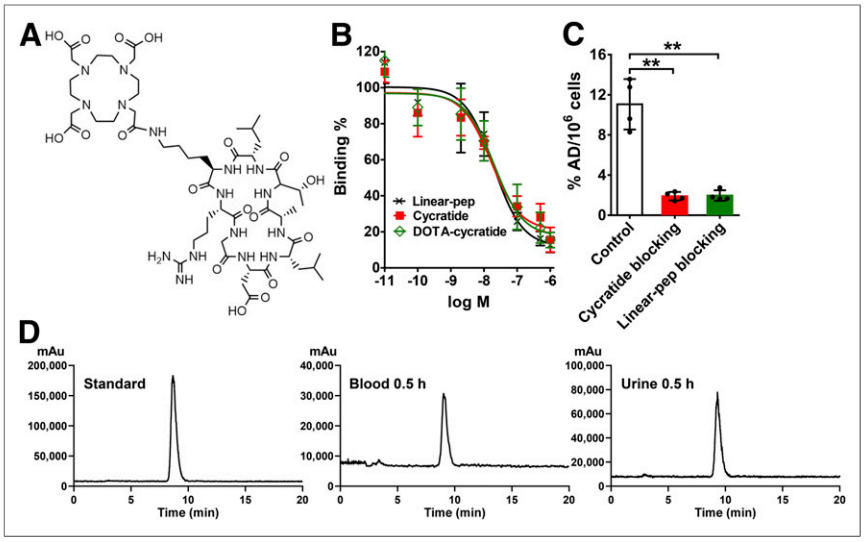

FIGURE 1. (A) Chemical structure of DOTA-cycratide. (B) Inhibition of ^{64}Cu-cycratide binding to integrin $\alpha_v\beta_6$ on BxPC-3 cells by cycratide, DOTA-cycratide, and linear-pep. Data are shown as mean ± SD, $n = 4$. (C) Binding of ^{68}Ga-cycratide to BxPC-3 with or without blocking of cold cycratide or linear-pep. %AD/10^6 cells = percentage of total added dose per million cells. Data are shown as mean ± SD, $n = 4$. (D) Metabolic stability of ^{68}Ga-cycratide in blood and urine of BALB/c mice (data are representative of 3 independent experiments). $^{**}P < 0.01$.

radiochemical purity higher than 85% after 4 h (Supplemental Fig. 1B).

In Vitro Cell-Binding Studies

The 50% inhibitory concentrations of cycratide (16.30 ± 2.36 nM), DOTA-cycratide (20.17 ± 1.68 nM), and linear-pep (19.58 ± 2.49 nM) were comparable (Fig. 1B). The binding values of ^{68}Ga-cycratide to BxPC-3 cells (percentage added dose per 10^6 cells) were significantly inhibited by the addition of excess doses of cycratide (11.06 ± 2.51 vs. 1.90 ± 0.41; $n = 4$, $P < 0.01$) or linear-pep (11.06 ± 2.51 vs. 1.96 ± 0.53; $n = 4$, $P < 0.01$; Fig. 1C).

In Vivo Metabolic Stability

The linear peptide radiotracer ^{68}Ga-linear-pep was rapidly metabolized after injection, with almost no intact peptide present in the blood or urine at 0.5 h after injection (Supplemental Fig. 1C). In contrast, the cyclic radiotracer ^{68}Ga-cycratide showed favorable metabolic stability in vivo, with no evident metabolites in the blood or urine at 0.5 h after injection (Fig. 1D).

Small-Animal PET Imaging and Biodistribution

The BxPC-3 tumors could be clearly visualized, with good tumor-to-background contrast, for ^{68}Ga-cycratide at 0.5 and 1 h but rapidly cleared, with low tumor uptake at 2 h (Fig. 2A). The region-of-interest–derived tumor uptake of ^{68}Ga-cycratide was significantly higher than that of ^{68}Ga-linear-pep at 0.5 h (3.82 ± 1.44 vs. 1.40 ± 0.38 %ID/g; $n = 4$, $P < 0.01$) and 1 h after injection (2.47 ± 1.18 vs. 0.90 ± 0.16 %ID/g; $n = 4$, $P < 0.01$). The tumor-to-muscle ratio for ^{68}Ga-cycratide was also significantly higher than that for ^{68}Ga-linear-pep at 0.5 h (4.77 ± 1.62 vs. 2.27 ± 0.63; $n = 4$, $P < 0.05$) and 1 h after injection (4.19 ± 1.29 vs. 2.27 ± 0.53; $n = 4$, $P < 0.05$; Fig. 2B).

To validate the PET imaging results, biodistribution studies were performed. As shown in Figure 2C, the tumor uptake of ^{68}Ga-cycratide was significantly higher than that of ^{68}Ga-linear-pep (2.15 ± 0.46 vs. 0.94 ± 0.58 %ID/g; $n = 4$, $P < 0.05$) at 0.5 h after injection. The tumor uptake of ^{68}Ga-cycratid was reduced significantly from 2.15 ± 0.46 to 1.10 ± 0.18 %ID/g at 0.5 h after injection ($n = 4$, $P < 0.01$) after blocking with cold cycratide.

Orthotopic BxPC-3 tumor lesions in the pancreas were clearly detected by ^{68}Ga-cycratide, with high contrast (Fig. 3A). A 74% reduction in the calculated %ID/g uptake of ^{68}Ga-cycratide was observed in the pancreas after blocking (Fig. 3A). After PET imaging, the presence of tumor lesions in the pancreas was verified by hematoxylin and eosin staining (Fig. 3B), and immunofluorescence staining further confirmed the positive expression of integrin $\alpha_v\beta_6$ in the tumor lesions (Fig. 3C).

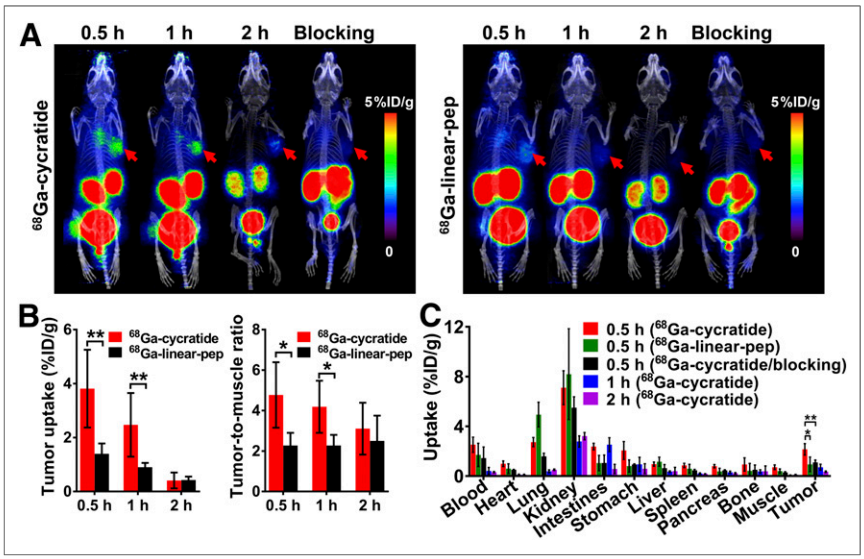

FIGURE 2. (A) Small-animal PET images obtained at 0.5, 1, and 2 h after injection of ^{68}Ga-cycratide or ^{68}Ga-linear-pep in BxPC-3 tumor–bearing mice without or with blocking doses of cold cycratide or linear-pep. Tumors are indicated by arrows. (B) Quantification of tumor uptake and tumor-to-muscle ratio of ^{68}Ga-cycratide and ^{68}Ga-linear-pep shown in A. Data are shown as mean ± SD, $n = 4$. (C) Biodistribution of ^{68}Ga-cycratide or ^{68}Ga-DOTA-linear-pep in BxPC-3 tumor–bearing mice without or with blocking dose of cold cycratide. Data are shown as mean ± SD, $n = 4$. $^{*}P < 0.05$. $^{**}P < 0.01$.

Biodistribution and Dosimetry of ^{68}Ga-Cycratide in Healthy Volunteers

No adverse events or obvious changes in signs or the results of clinical laboratory tests were found for any of the volunteers during the PET imaging procedure or within

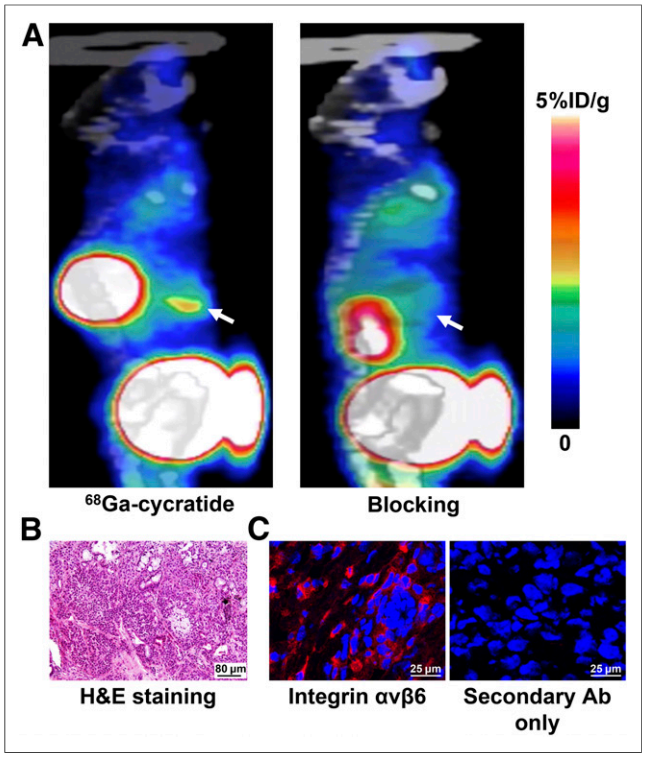

FIGURE 3. (A) PET imaging of orthotopic pancreatic cancer lesions in nude mice at 0.5 h after injection of ^{68}Ga-cycratide without or with blocking dose of cold cycratide. Tumors are indicated by arrows. (B) Hematoxylin and eosin (H&E) staining of tumor tissues harvested from orthotopic tumor model. (C) Left, immunofluorescence staining of integrin $\alpha_v\beta_6$ from tumor tissues harvested from orthotopic tumor model. Right, negative control with secondary antibody only.

2 wk after injection of ^{68}Ga-cycratide. The kidney and bladder showed the highest radioactivity accumulation, whereas the heart, liver, and spleen had relatively low activity (Fig. 4). The highest SUVs were observed in the kidney at all time points examined. The uptake of ^{68}Ga-cycratide in other organs, such as the lung, intestine, bone marrow, brain, and muscle, was relatively low (Supplemental Table 1).

The estimated absorbed radiation doses derived from the PET/CT images for each organ of the 5 volunteers are listed in Supplemental Table 2. The whole-body effective dose was 5.49E−02 ± 4.69E−02 mSv/MBq. The highest absorbed doses were in the urinary bladder wall (5.59E−01 ± 6.40E−01 mGy/MBq), as ^{68}Ga-cycratide was excreted predominantly via the renal route. The organs next to the urinary bladder walls and the kidneys, such as the ovaries and the uterus, also showed high absorbed doses.

PET Imaging of ^{68}Ga-Cycratide in Patients with Pancreatic Cancer

In a 55-y-old woman, uptake of ^{68}Ga-cycratide was evident in the region of the pancreatic mass, with an SUV_{max} of 4.86, and ^{18}F-FDG also showed a high accumulation of radioactivity in that region, with an SUV_{max} of 6.90 (Fig. 5A). After surgery and pathologic examination, this patient was later confirmed to have moderately differentiated pancreatic ductal adenocarcinoma (stage pT3N1). Immunohistochemical examination confirmed the expression of integrin $\alpha_v\beta_6$ in the tumor lesion (Fig. 5B).

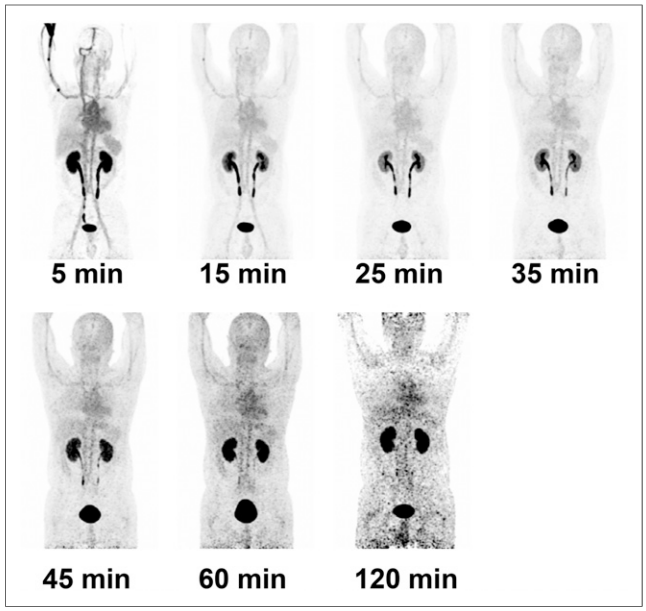

FIGURE 4. Multiple-time-point whole-body maximum-intensity-projection PET images of male healthy volunteer after injection of ^{68}Ga-cycratide.

Another patient (a 54-y-old man) had been previously diagnosed with pancreatic cancer. This patient had undergone surgery 7 mo before and 7 periods of chemotherapy (gemcitabine plus tegafur, gimeracil, and oteracil potassium capsules) after surgery. Retroperitoneal soft-tissue masses were observed on enhanced-CT examination (Fig. 5C). ^{68}Ga-cycratide showed a low uptake with an SUV_{max} of 1.6 and an SUV_{mean} of 0.9, and ^{18}F-FDG exhibited an SUV_{max} of 2.2 and an SUV_{mean} of 1.8 in the pancreas. After 3 mo, enhanced CT was performed again, and the mass was markedly reduced (Fig. 5C), suggesting an inflammatory reaction rather than a tumor relapse.

DISCUSSION

Herein, we prepared a novel ^{68}Ga-radiolabeled cyclic peptide targeting integrin $\alpha_v\beta_6$, tested it in a preclinical orthotopic model, investigated its biodistribution and dosimetry profile in healthy volunteers, and performed preliminary clinical PET imaging on patients with pancreatic cancer. We found that ^{68}Ga-cycratide is an integrin $\alpha_v\beta_6$–specific PET radiotracer that can be easily prepared and has a favorable pharmacokinetics and dosimetry profile.

The introduction of NOTA-Al^{18}F chelating strategy has markedly simplified the preparation of ^{18}F-labeled peptides, with potential kit formulation for clinical application (*30*). We prepared the ^{18}F-labeled NOTA-cycratide with high purity by using Al^{18}F (Supplemental Fig. 2) and observed that the in vitro tumor cell uptake pattern for ^{18}F-cycratide was comparable to that for ^{68}Ga-cycratide (Supplemental Fig. 3). However, compared with ^{68}Ga-cycratide, evident radioactivity uptake in the spine was observed 2 h after injection of ^{18}F-cycratide (Supplemental Fig. 4). The biodistribution showed that the uptake of ^{18}F-cycratide in the bone increased with time from 0.5 to 2 h (Supplemental Fig. 5). Compared with ^{68}Ga-cycratide, a significantly higher uptake in the kidney, bone, and muscle at 1 and 2 h after injection, and a significantly lower tumor-to-muscle ratio at 0.5, 1, and 2 h after injection, was observed for ^{18}F-cycratide ($P < 0.05$; $n = 4$; Supplemental Fig. 6). Therefore, the superior in vitro characterization and in vivo behaviors of ^{68}Ga-cycratide as compared with the ^{18}F-labeled counterpart (Supplemental Table 3), as well as its easy availability, facilitate its use in clinical settings.

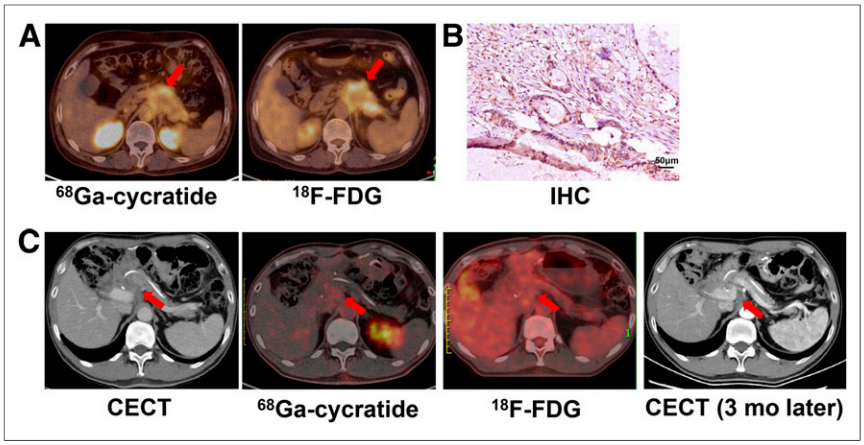

FIGURE 5. (A) PET/CT images of female patient with suspected pancreatic cancer. Images were obtained at 1 h after intravenous administration of ^{68}Ga-cycratide or ^{18}F-FDG. Tumors are indicated by arrows. (B) Immunohistochemical (IHC) staining for integrin $\alpha_v\beta_6$ in tumor sample from same patient as in A. (C) Contrast-enhanced CT (CECT) image and PET/CT images of male patient with pancreatic cancer 7 mo after surgery at 1 h after administration of ^{68}Ga-cycratide or ^{18}F-FDG, as well as CECT image of same patient 3 mo later (10 mo after surgery). Occupancy lesions in CT are indicated by arrows.

We therefore tested the in vivo behavior of ^{68}Ga-cycratide in healthy volunteers. Dynamic scan results showed that ^{68}Ga-cycratide was cleared via renal and bladder routes, and background in the blood and surrounding abdominal organs was quite low, which would allow for sensitive detection of pancreatic tumor lesions. Notably, background uptake in the abdomen and intestine were much lower than recently reported for a ^{68}Ga-labeled integrin $\alpha_v\beta_6$–targeting radiotracer in humans (*22,23*); this difference may have resulted at least in part from the improved in vivo stability of ^{68}Ga-cycratide. The dosimetry of ^{68}Ga-cycratide was comparable to that of other ^{68}Ga-labeled peptides (*31,32*), and no adverse events or abnormal vital signs or clinical laboratory test results were observed after injection, confirming that ^{68}Ga-cycratide is safe and well tolerated in healthy volunteers.

^{68}Ga-cycratide and ^{18}F-FDG imaging both confirmed the advantages of ^{18}F-FDG and ^{68}Ga-cycratide over enhanced CT for monitoring postsurgery relapse (Fig. 5C). In a patient with suspected pancreatic cancer, both ^{68}Ga-cycratide and ^{18}F-FDG were able to identify the lesions (Fig. 5A). Although the SUV for ^{68}Ga-cycratide was slightly lower than that for ^{18}F-FDG, immunohistochemical analysis confirmed integrin-specific targeting of ^{68}Ga-cycratide (Fig. 5B). Despite the fact that ^{18}F-FDG is more sensitive than CT, ^{18}F-FDG suffers from false-positive uptake in the presence of focal mass-forming pancreatitis (*4,33*). Altmann et al. demonstrated that ^{68}Ga-labeled integrin $\alpha_v\beta_6$–targeting peptides are more specific for the differentiation of lung cancer from inflammation than is ^{18}F-FDG (*22*), and integrin $\alpha_v\beta_6$–targeted PET imaging can sensitively detect a variety of metastasis sites, including the lungs, liver, bone, and brain (*13*). Indeed, in our animal studies, side-by-side comparison of the PET images of ^{68}Ga-cycratide and ^{18}F-FDG demonstrated that integrin $\alpha_v\beta_6$–specific imaging using ^{68}Ga-cycratide holds potential advantages over ^{18}F-FDG for the differentiation of tumors (Supplemental Fig. 7). Because integrin $\alpha_v\beta_6$ and transforming growth factor β affect the tumor suppressor pathway to promote pancreatic cancer progression (*34*), additional investigation into the correlation of ^{68}Ga-cycratide uptake with integrin $\alpha_v\beta_6$ expression, as well as tumor progression, is warranted to further demonstrate the role of ^{68}Ga-cycratide in noninvasive pancreatic cancer PET staging.

This study had several limitations. First, tumor uptake of ^{68}Ga-cycratide was relatively low (~2 %ID/g; Fig. 2C). The integrin $\alpha_v\beta_6$–binding affinity of ^{68}Ga-cycratide could be further improved to increase the tumor uptake and retention, which may result in higher SUVs in humans. We tested the multimerization strategy by construction of a dimeric cycratide; however, the receptor-binding affinity and tumor uptake did not show evident improvement, consistent with observations by Notni et al. (*16*). Therefore, optimization strategies other than multimerization may be needed in future studies. Further, we tested PET imaging of ^{68}Ga-cycratide in only 2 patients with pancreatic cancer. This is a very small sample size, and further large-scale prospective clinical studies comparing ^{68}Ga-cycratide and ^{18}F-FDG, as well as studies correlating the SUV of ^{68}Ga-cycratide with integrin $\alpha_v\beta_6$ expression levels, are necessary to evaluate the full potential of ^{68}Ga-cycratide in pancreatic cancer detection, staging, and prognosis monitoring.

CONCLUSION

The cyclic radiotracer ^{68}Ga-cycratide showed high targeting specificity for integrin $\alpha_v\beta_6$ in vitro and in pancreatic cancer mouse models. Pilot clinical studies demonstrated that this radiotracer is safe and can specifically detect pancreatic cancer and monitor therapy. Larger-scale clinical trials of ^{68}Ga-cycratide and comparisons to ^{18}F-FDG are warranted to further characterize the utility of ^{68}Ga-cycratide for detection or treatment monitoring in patients with pancreatic cancer.

DISCLOSURE

This work was supported by the National Key R&D Program of China (2018YFE0205300 and 2018YFC1313300), the National Natural Science Foundation of China (81671747, 81873907, and 81920108020), the Beijing Nova Program Interdisciplinary Cooperation Project (Z181100006218136), the Beijing Natural Science Foundation (L172007 and JQ19026), and the Clinical Medicine Plus X–Young Scholars Project of Peking University (PKU2019LCXQ023). No other potential conflict of interest relevant to this article was reported.

KEY POINTS

QUESTION: Can the integrin $\alpha_v\beta_6$–targeting cyclic peptide radiotracer ^{68}Ga-cycratide be used for PET imaging of pancreatic cancer in the clinic?

PERTINENT FINDINGS: ^{68}Ga-cycratide can be rapidly prepared with high radiochemical purity and has favorable in vivo pharmacokinetics. It is safe and has a favorable dosimetry profile. PET imaging using ^{68}Ga-cycratide can detect integrin $\alpha_v\beta_6$–positive lesions in patients with pancreatic cancer.

IMPLICATIONS FOR PATIENT CARE: ^{68}Ga-cycratide is clinically translatable for PET imaging of pancreatic cancer and may also be extended to enable treatment response monitoring and prognosis staging.

REFERENCES

1. Ryan DP, Hong TS, Bardeesy N. Pancreatic adenocarcinoma. *N Engl J Med.* 2014;371:1039–1049.
2. Vincent A, Herman J, Schulick R, Hruban RH, Goggins M. Pancreatic cancer. *Lancet.* 2011;378:607–620.
3. Tummala P, Junaidi O, Agarwal B. Imaging of pancreatic cancer: an overview. *J Gastrointest Oncol.* 2011;2:168–174.
4. Dimastromatteo J, Brentnall T, Kelly KA. Imaging in pancreatic disease. *Nat Rev Gastroenterol Hepatol.* 2017;14:97–109.
5. Yeh R, Steinman J, Luk L, Kluger MD, Hecht EM. Imaging of pancreatic cancer: what the surgeon wants to know. *Clin Imaging.* 2017;42:203–217.
6. Tamm EP, Balachandran A, Bhosale PR, et al. Imaging of pancreatic adenocarcinoma: update on staging/resectability. *Radiol Clin North Am.* 2012;50:407–428.
7. Salmon E, Ir CB, Hustinx R. Pitfalls and limitations of PET/CT in brain imaging. *Semin Nucl Med.* 2015;45:541–551.
8. Tagliabue L, Del Sole A. Appropriate use of positron emission tomography with [^{18}F]fluorodeoxyglucose for staging of oncology patients. *Eur J Intern Med.* 2014;25:6–11.
9. Kadhim LA, Dholakia AS, Herman JM, Wahl RL, Chaudhry MA. The role of ^{18}F-fluorodeoxyglucose positron emission tomography in the management of patients with pancreatic adenocarcinoma. *J Radiat Oncol.* 2013;2:341–352.
10. Bandyopadhyay A, Raghavan S. Defining the role of integrin $\alpha_v\beta_6$ in cancer. *Curr Drug Targets.* 2009;10:645–652.
11. Gao D, Gao L, Zhang C, et al. A near-infrared phthalocyanine dye-labeled agent for integrin $\alpha_v\beta_6$-targeted theranostics of pancreatic cancer. *Biomaterials.* 2015; 53:229–238.
12. Hausner SH, DiCara D, Marik J, Marshall JF, Sutcliffe JL. Use of a peptide derived from foot-and-mouth disease virus for the noninvasive imaging of human cancer: generation and evaluation of 4-[^{18}F]fluorobenzoyl A20FMDV2 for in vivo imaging of integrin alphavbeta6 expression with positron emission tomography. *Cancer Res.* 2007;67:7833–7840.
13. Hausner SH, Bold RJ, Cheuy LY, et al. Preclinical development and first-in-human imaging of the integrin $\alpha_v\beta_6$ with [^{18}F]$\alpha_v\beta_6$-binding peptide in metastatic carcinoma. *Clin Cancer Res.* 2019;25:1206–1215.
14. Kimura RH, Teed R, Hackel BJ, et al. Pharmacokinetically stabilized cystine knot peptides that bind $\alpha_v\beta_6$ integrin with single-digit nanomolar affinities for detection of pancreatic cancer. *Clin Cancer Res.* 2012;18:839–849.
15. Hackel BJ, Kimura RH, Miao Z, et al. ^{18}F-fluorobenzoate-labeled cystine knot peptides for PET imaging of integrin $\alpha_v\beta_6$. *J Nucl Med.* 2013;54:1101–1105.
16. Notni J, Reich D, Maltsev OV, et al. In vivo PET imaging of the cancer integrin $\alpha_v\beta_6$ using ^{68}Ga-labeled cyclic RGD nonapeptides. *J Nucl Med.* 2017;58:671–677.
17. Keat N, Kenny J, Chen K, et al. A microdose PET study of the safety, immunogenicity, biodistribution, and radiation dosimetry of ^{18}F-FB-A20FMDV2 for imaging the integrin $\alpha_v\beta_6$. *J Nucl Med Technol.* 2018;46:136–143.
18. Saha A, Ellison D, Thomas GJ, et al. High-resolution in vivo imaging of breast cancer by targeting the pro-invasive integrin $\alpha_v\beta_6$. *J Pathol.* 2010;222:52–63.
19. Zhu X, Li J, Hong Y, et al. ^{99m}Tc-labeled cystine knot peptide targeting integrin $\alpha_v\beta_6$ for tumor SPECT imaging. *Mol Pharm.* 2014;11:1208–1217.
20. Liu Z, Liu H, Ma T, et al. Integrin $\alpha_v\beta_6$-targeted SPECT imaging for pancreatic cancer detection. *J Nucl Med.* 2014;55:989–994.
21. Liu H, Wu Y, Wang F, Liu Z. Molecular imaging of integrin $\alpha_v\beta_6$ expression in living subjects. *Am J Nucl Med Mol Imaging.* 2014;4:333–345.
22. Altmann A, Sauter M, Roesch S, et al. Identification of a novel ITG$\alpha_v\beta_6$-binding peptide using protein separation and phage display. *Clin Cancer Res.* 2017;23: 4170–4180.
23. Roesch S, Lindner T, Sauter M, et al. Comparison of the RGD motif-containing $\alpha_v\beta_6$ integrin-binding peptides SFLAP3 and SFITGv6 for diagnostic application in HNSCC. *J Nucl Med.* 2018;59:1679–1685.
24. Flechsig P, Lindner T, Loktev A, et al. PET/CT imaging of NSCLC with a $\alpha_v\beta_6$ integrin-targeting peptide. *Mol Imaging Biol.* 2019;21:973–983.
25. Gao L, Zhang C, Gao D, et al. Enhanced anti-tumor efficacy through a combination of integrin $\alpha_v\beta_6$-targeted photodynamic therapy and immune checkpoint inhibition. *Theranostics.* 2016;6:627–637.
26. Yu X, Gao D, Gao L, et al. Inhibiting metastasis and preventing tumor relapse by triggering host immunity with tumor-targeted photodynamic therapy using photosensitizer-loaded functional nanographenes. *ACS Nano.* 2017;11:10147–10158.
27. Liu S. Radiolabeled cyclic RGD peptide bioconjugates as radiotracers targeting multiple integrins. *Bioconjug Chem.* 2015;26:1413–1438.
28. Liu Z, Wang F. Development of RGD-based radiotracers for tumor imaging and therapy: translating from bench to bedside. *Curr Mol Med.* 2013;13:1487–1505.
29. Liu H, Gao L, Yu X, et al. Small-animal SPECT/CT imaging of cancer xenografts and pulmonary fibrosis using a ^{99m}Tc-labeled integrin $\alpha_v\beta_6$-targeting cyclic peptide with improved in vivo stability. *Biophys Rep.* 2018;4:254–264.
30. McBride WJ, Sharkey RM, Karacay H, et al. A novel method of ^{18}F radiolabeling for PET. *J Nucl Med.* 2009;50:991–998.
31. Zhang J, Lang L, Zhu Z, Li F, Niu G, Chen X. Clinical translation of an albumin-binding PET radiotracer ^{68}Ga-NEB. *J Nucl Med.* 2015;56:1609–1614.
32. Zhang J, Niu G, Fan X, et al. PET using a GRPR antagonist ^{68}Ga-RM26 in healthy volunteers and prostate cancer patients. *J Nucl Med.* 2018;59:922–928.
33. Buck AC, Schirrmeister HH, Guhlmann CA, et al. Ki-67 immunostaining in pancreatic cancer and chronic active pancreatitis: does in vivo FDG uptake correlate with proliferative activity? *J Nucl Med.* 2001;42:721–725.
34. Hezel AF, Deshpande V, Zimmerman SM, et al. TGF-beta and $\alpha_v\beta_6$ integrin act in a common pathway to suppress pancreatic cancer progression. *Cancer Res.* 2012;72:4840–4845.